NIH Public Access
Author Manuscript
*Cell*. Author manuscript; available in PMC 2014 February 28.

Published in final edited form as:
*Cell*. 2013 February 28; 152(5): 1037–1050. doi:10.1016/j.cell.2013.02.006.

# Jmjd3 Negatively Regulates Reprogramming Through Histone Demethylase Activity- Dependent and -Independent Pathways

**Wei Zhao**[1], **Qingtian Li**[1], **Stephen Ayers**[2], **Yifeng Gu**[1], **Zhong Shi**[3], **Yidong Chen**[4], **Helen Y. Wang**[1], and **Rong-Fu Wang**[1,*]

[1]Center for Inflammation and Epigenetics, The Methodist Hospital Research Institute, Houston, Texas 77030, USA

[2]Genomic Medicine, The Methodist Hospital Research Institute, Houston, Texas 77030, USA

[3]The Center for Cell and Gene Therapy, Baylor College of Medicine, Houston, Texas 77030, USA

[4]Department of Epidemiology and Biostatistics and Greehey Children's Cancer Research Institute, The University of Texas Health Science Center at San Antonio, San Antonio, Texas 78229, USA

## Abstract

Although somatic cell reprogramming to generate inducible pluripotent stem cells (iPSCs) is associated with profound epigenetic changes, the roles and mechanisms of epigenetic factors in this process remain poorly understood. Here we identify Jmjd3 as a potent negative regulator of reprogramming. *Jmjd3*-deficient MEFs produced significantly more iPSC colonies than did wild-type cells, while ectopic expression of *Jmjd3* markedly inhibited reprogramming. We show that the inhibitory effects of Jmjd3 are produced through both histone demethylase-dependent and -independent pathways. The latter pathway is entirely novel and involves Jmjd3 targeting of PHF20 for ubiquitination and degradation via recruitment of an E3 ligase, Trim26. Importantly, *PHF20*-deficient MEFs could not be converted to fully reprogrammed iPSCs, even with knockdown of *Jmjd3*, *Ink4a* or *p21*, indicating that this protein exerts predominant effects on reprogramming. Our findings demonstrate a previously unrecognized role of Jmjd3 in cellular reprogramming and provide molecular insight into the mechanisms by which the Jmjd3-PHF20 axis controls this process.

## Introduction

Both human and mouse somatic cells can be reprogrammed to a pluripotent embryonic stem cell (ESC)-like state, giving rise to induced pluripotent stem cells (iPSCs), by the use of four key transcription factors: Oct4, Sox2, Klf4 and c-Myc (Takahashi et al., 2007b; Takahashi and Yamanaka, 2006; Yu et al., 2007). Because of their similarity to ESCs in terms of gene expression profile, epigenetics/genetic marks, and their ability to self-renew and differentiate into many different cell types, iPSCs hold great promise for human disease modeling, drug screening and perhaps therapeutic applications (Robinton and Daley, 2012;

© 2013 Elsevier Inc. All rights reserved.

*Correspondence: rwang3@tmhs.org.

Supplemental Information: Supplemental Information includes Extended Experimental Procedures, seven supplemental Figures and three Tables and can be found with this article online.

**Publisher's Disclaimer:** This is a PDF file of an unedited manuscript that has been accepted for publication. As a service to our customers we are providing this early version of the manuscript. The manuscript will undergo copyediting, typesetting, and review of the resulting proof before it is published in its final citable form. Please note that during the production process errors may be discovered which could affect the content, and all legal disclaimers that apply to the journal pertain.

NIH-PA Author Manuscript
NIH-PA Author Manuscript
NIH-PA Author Manuscript

NIH-PA Author Manuscript

NIH-PA Author Manuscript

NIH-PA Author Manuscript

Stadtfeld and Hochedlinger, 2010). Although somatic cell reprogramming can be achieved by several strategies (Hanna et al., 2009; Robinton and Daley, 2012; Stadtfeld and Hochedlinger, 2010), its efficiency and the kinetics of iPSC generation are still suboptimal, suggesting the existence of substantial genetic and epigenetic barriers during reprogramming.

Many factors, including cell proliferation and cycling, mesenchymal-to-epithelial transitions and epigenetic regulation of histone modification and DNA methylation, influence reprogramming efficiency (Plath and Lowry, 2011; Stadtfeld and Hochedlinger, 2010). Transiently enforced expression of reprogramming factors leads to separable events, beginning with mesenchymal-to-epithelial transitions associated with loss of the somatic marker THY1, followed by the activation of embryonic markers such as alkaline phosphatase (AP) and stage-specific embryonic antigen 1 (SSEA1) (Li et al., 2010; Plath and Lowry, 2011). Induction and maintenance of endogenous pluripotency genes such as *Nanog* and *Oct4* require further epigenetic reprogramming changes at the DNA methylation and histone modification levels (Stadtfeld and Hochedlinger, 2010). Failure to achieve these epigenetic changes in a timely manner can lead to partially reprogrammed iPSCs.

Global analysis of euchromatin dynamics during the reprogramming process has revealed orchestrated epigenetic changes at the histone modification level (Gaspar-Maia et al., 2011; Hemberger et al., 2009; Koche et al., 2011). Both ESCs and iPSCs contain “bivalent domains”, where nucleosomes are marked with trimethylation at histone3-lysine27 (H3K27me3) and histone3-lysine4 (H3K4me3) (Gaspar-Maia et al., 2011). While the Polycomb group (PcG) complex mediates H3K27 methylation and inhibits gene repression (Margueron and Reinberg, 2011), Jmjd3 and Utx mediate H3K27 demethylation (Agger et al., 2007; Lan et al., 2007). Thus, given the importance of epigenetic factors in defining cell lineages, it is reasonable to suggest that some of these factors are required for efficient somatic reprogramming, while others may function as negative regulators. Removal of such roadblocks to successful reprogramming will require increased insight into the molecular mechanisms by which epigenetic factors control cell lineage and hence the dynamic process of reprogramming. Here we report identification of Jmjd3 as a potent negative regulator of somatic cell reprogramming in screening studies of a panel of histone-modifying proteins. Knockdown or ablation of Jmjd3 enhanced the efficiency and kinetics of reprogramming, apparently by dual mechanisms: 1) Jmjd3 partially inhibits iPSC reprogramming by promoting cell senescence through upregulation of *p21* and *Ink4a*, and 2) Jmjd3 targets PHF20 (plant homeodomain finger protein 20) for ubiquitination and proteasomal degradation via the E3 ubiquintin ligase Trim26 in a demethylase activity-independent manner. Knockdown or ablation of PHF20 blocks the reactivation of endogenous *Oct4* expression, thus leading to partially programmed cells. Our results implicate the Jmjd3-PHF20 axis as a key pathway in somatic cell reprogramming, and provide novel insights into the molecular mechanisms used by Jmjd3 to impede efficient reprogramming.

## Results

### Identification of Jmjd3 as an Inhibitor of Reprogramming

To establish a simpler and inducible 4F-based method to generate iPSCs, we created transgenic mice expressing tetracycline (Tet)-O-inducible *Oct4*, *Sox2*, *Klf4* and *Myc* transgenic mice carrying rtTA-M2 reverse tetracycline transactivator (Figure 1A). Mouse embryonic fibroblasts (MEFs) were generated from intercrossing transgenic mice (Figure S1A). As shown in Figure 1B, Oct4, Sox2, Klf4, and Myc proteins were readily detected by immunoblot analysis after treatment with Dox for 24 h. These 4F-expressing MEFs (Tet-O-4F MEFs) could be efficiently reprogrammed to generate iPSCs in the presence of Dox (Figure 1C). Withdrawal of Dox before or at day 8 markedly reduced $AP^+$ colony formation,

NIH-PA Author Manuscript

NIH-PA Author Manuscript

NIH-PA Author Manuscript

but withdrawn at day 10 or later showed little or no effect on $AP^+$ colony number using three different types of MEFs (WT, Tet-O-4F and Oct4-GFP) (Figure S1B-D). The fully programmed iPSCs stained positively for AP, SSEA-1 and Nanog (Figures 1D-G), suggesting that Tet-O-4F MEF-based reprogramming would provide a reliable system to screen for epigenetic factors that either enhance or reduce the efficiency of reprogramming.

We predicted that epigenetic factors play critical roles in reactivating the expression of stem cell-enriched genes, while shutting down the expression of cell lineage-specific differentiation genes, thus greatly increasing the efficiency of 4F-mediated reprogramming. To test this notion, we selected a panel of shRNAs with high knockdown efficiency (>70%) against a subset of genes encoding histone methyltransferases or demethylases based on PCR or western blot analysis (Figures S1E-S1F and Tables S1-S2). After three rounds of screening, we found that knockdown of the H3K27 methyltransferase *Ezh2* and many histone demethylase genes, including *Fbxl10*, *Jarid1b*, *Jarid1d*, *Jarid2*, *Jmjd1a*, *Jmjd2c* and *Utx*, markedly decreased reprogramming efficiency (Figure 1H), consistent with recent findings for *Utx* and *Fbxl10* (Mansour et al., 2012; Wang et al., 2011). By contrast, knockdown of *Jmjd3* markedly increased the efficiency of 4F-mediated reprogramming, while its ectopic expression resulted in decreased reprogramming efficiency (Figure 1I), suggesting that Jmjd3 functions as a barrier to somatic reprogramming. This unique feature of Jmjd3 led to its selection for further study.

## *Jmjd3* Ablation Enhances the Efficiency and Kinetics of Reprogramming

To further define the role of Jmjd3 in reprogramming, we generated *Jmjd3* knockout mice by targeted deletion of exon 15-21 using a Cre-LoxP system (Figure 2A). Global deletion of *Jmjd3* died shortly after birth due to lung dysfunction (to be reported elsewhere). Expression of *Jmjd3* was abrogated in *Jmjd3*-deficient MEFs (Figure 2A). Consistent with results obtained by *Jmjd3* knockdown, 4F-reprogramming of *Jmjd3*-deficienct MEFs produced significantly more iPSC colonies than did WT MEFs (Figure 2B). Robust reprogramming was also achieved with *Jmjd3*-deficient 3F-transduced MEFs (Oct4, Sox2 and Klf4), compared with WT MEFs (Figure 2B). By contrast, *Ezh2*-deficient MEFs, which were generated by treating $Ezh_2^{flox/flox}$:Cre-ESR MEFs with tamoxifen, strikingly inhibited the efficiency of 4F-mediated reprogramming of MEFs (Figure 2C), further confirming that *Ezh2* is necessary for reprogramming. More importantly, we found that $AP^+$ iPSC colonies appeared much earlier in *Jmjd3*-deficient MEFs than in WT MEFs (Figure 2D). The iPSCs generated from *Jmjd3*-deficient MEFs showed characteristic ESC morphology and markers such as AP, SSEA-1 and Nanog (Figures 2E-2G). They also formed teratomas comprising all three embryonic germ layers (ectoderm, mesoderm and endoderm) (Figures 2H-2I), and contributed to chimeras after injection into BALB/C host blastocysts (Figure 2J). Taken together, these results suggest that loss of *Jmjd3* markedly enhances the efficiency and kinetics of iPSC reprogramming.

## Jmjd3 Negatively Regulates Reprogramming by Modulating Expression of the *Ink4a/Arf* Locus

We next asked how *Jmjd3* ablation enhances reprogramming. *Jmjd3* expression is thought to increases the expression of *Ink4a/Arf* in MEFs by modifying H3K27 methylation in the promoter region of the *Ink4a/Arf* locus (Agger et al., 2009; Barradas et al., 2009). Knockdown or deletion of *Ink4a/Arf* and *p21* reduces cell senescence and markedly increases the efficiency of reprogramming (Hong et al., 2009; Kawamura et al., 2009; Li et al., 2009; Marion et al., 2009; Utikal et al., 2009). To assess the expression level of these molecules in *Jmjd3*-deficient MEFs, we showed that *Jmjd3* deletion markedly reduced the expression of *Ink4a*/*Arf* mRNA and protein (Figure 3A and Figure S2A). The p21 protein, but not its mRNA, was also reduced in *Jmjd3*-deficient MEFs (Figure 3A and Figure S2A).

NIH-PA Author Manuscript

NIH-PA Author Manuscript

NIH-PA Author Manuscript

Consistent with this, we found that *Jmjd3*-deficient MEF cells grew faster than WT cells and reduced cellular senescence based on β-galactosidase (β-gal) staining, compared with WT MEFs (Figures 3B-3C). Because the *Jmjd3*-deficient MEFs eventually underwent a senescence crisis after 5-7 passages, it is likely that transient effects of *Jmjd3* deficiency on cell proliferation and senescence may have contributed to the improved efficiency and kinetics of reprogramming.

To determine the relative contribution of downregulation of *Ink4a*/*Arf* and *p21* to increased efficiency of reprogramming in *Jmjd3*-deficient MEFs, we knocked down the expression of these genes with specific shRNAs (Figure S2B). Although knockdown of *Jmjd3*, *Ink4a/Arf* or *p21* alone by shRNAs increased reprogramming efficiency, compared to that in MEFs transduced with a control shRNA, the efficiency nearly doubled with simultaneous knockdown of *Jmjd3* and *Ink4a/Arf* or *p21* (Figure 3D), suggesting that Jmjd3 might have additional effects on reprogramming. To test this possibility, we generated the *Jmjd3-N* (containing the N-terminal 450 aa), *Jmjd3-ΔJmjC* (containing a deletion in the catalytic Jumonji domain) and *Jmjd3-H1390A* (containing a point mutation in the catalytic domain) constructs, all of which lack the H3K27me3 demethylase activity of H3K27 trimethylation (Figure S2C). To determine whether Jmjd3-mediated inhibition of reprogramming depends upon expression of *Ink4a/Arf* and *p21*, we showed that ectopic expression of full-length *Jmjd3*, but not *Jmjd3-N*, *Jmjd3-ΔJmjC* or *Jmjd3-H1390A*, in *Jmjd3*-deficient MEFs restored the expression of *Ink4a/Arf* (Figure 3E) and markedly inhibited reprogramming (Figure 3F). Surprisingly, two Jmjd3 mutants (*Jmjd3-ΔJmjC* and *Jmjd3-H1390A*) that lacked H3K27 demethylase activity and failed to upregulate *Ink4a/Arf* expression were still capable of inhibiting reprogramming in *Jmjd3*-deficient MEFs (Figure 3F), suggesting that Jmjd3 can modulate reprogramming through a previously unknown, demethylase activity-independent pathway.

## PHF20 is a Key Target of the Jmjd3 Protein

To search for the targets of Jmjd3, we performed a comparative analysis of miRNA and mRNA gene expression between WT and *Jmjd3*-deficient MEFs, but failed to identify any gene that could be responsible for the increased reprogramming efficiency in *Jmjd3*-deficient MEF cells (data not shown). Hence, we turned our attention to the expression levels of epigenetic factors, because they are critical in reprogramming somatic cells to an ESC-like state (Plath and Lowry, 2011; Stadtfeld and Hochedlinger, 2010). By comparing the expression of 59 genes that encode for histone modification proteins, we identified 18 genes that were markedly upregulated at the RNA level in iPSCs/ESCs, versus MEFs, and 11 genes that were upregulated between iPSCs/ESCs versus human fibroblasts (Figure S2D and S2E). Among them, seven genes were highly expressed in both mouse and human iPSCs/ESCs (Figure S2F). Of these, only PHF20 (also called GLEA2) showed a marked increase of expression in *Jmjd3*-deficient MEFs, iPSCs and ESCs, versus WT MEFs (Figure 3G). However, no appreciable differences in *PHF20* mRNA and H3K27 trimethylation were observed between WT and *Jmjd3*-deficient MEFs (Figure S3A-S3B). *PHF20* was strongly expressed in testis, ovary and ES cells, but weakly in other tissues (Figures S3C and S3D). Interestingly, PHF20 expression was gradually increased in WT MEFs during reprogramming, which was accelerated in *Jmjd3*-deficient MEFs (Figure 3H). These results suggest that the PHF20 protein is an important target of Jmjd3, and thus may play a role in ESCs and iPSCs.

## Requirement for PHF20 in the Maintenance and Reprogramming of ESCs and iPSCs

Because the PHF20 protein is abundantly expressed in both ESCs and iPSCs, we next sought to determine its importance in the maintenance of these cell types. After knocking down *PHF20* in ESCs with specific shRNAs containing a *GFP* cassette (Figure S4A), ESCs

NIH-PA Author Manuscript

NIH-PA Author Manuscript

NIH-PA Author Manuscript

underwent differentiation, while ESCs transduced with control shRNA remained undifferentiated (Figure 4A). Furthermore, RT-PCR and western blot analyses revealed that *PHF20* expression in ESCs, like that of *Oct4* and *Nanog*, was markedly reduced after withdrawal of leukemia-inhibiting factor (LIF) and addition of retinoic acid (RA) in the culture medium (Figure 4B and 4C). Similar results were obtained with iPSCs (Figures S4B and S4C). To determine whether stable ESC lines could be derived from WT and *PHF20* knockout mice, we found that ESC lines could be readily generated from WT mice, but not from *PHF20* knockout mice (Figure S4D-S4E). WT ESCs expressed AP, Nanog and Oct4 proteins, whereas cells from *PHF20* knockout blastocysts did not (Figure S4E) and differentiated rapidly into trophectoderm, based on downregulation of *Oct4* and upregulation of *Cdx2* (Figure S4F). These results suggest that PHF20 is required for the generation and maintenance of both ESCs and iPSCs.

To further define the role of PHF20 in iPSC generation, we first knocked down the protein in Tet-O-4F MEFs at different time points and tested its ability to form iPSC colonies. Knockdown of *PHF20* in the early stages of reprogramming (i.e., at day 0 or 4) markedly blocked iPSC generation, whereas in the intermediate or later stages (day 10 or 12) it led to a decreased (but still significant) inhibitory effect on the numbers of iPSC colonies (Figure 4D). Using *PHF20* knockout MEFs (Figure 4E), we showed that reprogramming to iPSCs with either 3F or 4F was significantly inhibited in *PHF20*-deficient MEFs (Figure 4F), and the few iPSC colonies that were generated from *PHF20*-deficient MEFs showed only partially reprogrammed iPSCs (Figure 4G), suggesting that PHF20 is required for the efficient generation of fully reprogrammed iPSCs.

Like the results obtained with *Jmjd3*-deficient MEFs, we found that *Jmjd3* knockdown in human fibroblasts enhanced reprogramming, while *PHF20* knockdown blocked this process (Figure S4G and S4H). To clarify how Jmjd3 and PHF20 reciprocally regulate reprogramming, we generated *Jmjd3/PHF20* single- or double-knockout MEFs and tested their ability to regulate reprogramming. Both *Jmjd3*-deficient and *Jmjd3/PHF20* double-knockout MEF cells grew faster than WT and *PHF20*-deficient cells, but no appreciable difference was observed in the growth between WT and *PHF20*-deficient cells (Figure S4I). As expected, *Jmjd3* deletion enhanced reprogramming, but *PHF20* ablation inhibited this process (Figure 4H). Remarkably, *Jmjd3* deletion failed to improve reprogramming in *Jmjd3* and *PHF20* double-knockout MEFs (Figure 4H), suggesting that the proliferative advantage of *Jmjd3*-deficient MEFs cannot overcome the failure of reprogramming in *PHF20*-deficient MEFs. Similar results were obtained when either *Ink4a* or *p21* was knocked down in *PHF20*-deficient MEFs: that is, loss of each of these regulators increased reprogramming in WT MEFs, but failed to rescue defective reprogramming in *PHF20*-deficient MEFs (Figure 4I). Ectopic expression of *PHF20*, by contrast, restored reprogramming in *PHF20*-deficient MEFs (Figure 4J), suggesting a requirement for expression of this gene in both WT and *Jmjd3*-deficient MEFs.

To further examine the ability of *PHF20* expression to facilitate reprogramming, we generated Tet-O-*PHF2*0 MEFs from *rtTA*:Tet-O-*PHF20* transgenic mice and treated them with Dox, resulting in increased expression of PHF20, compared with findings in Dox-treated *rtTA*-expressing WT MEFs (Figure 4K). More importantly we observed that Dox-induced expression of *PHF20* in these cells led to a marked increase in the efficiency of 4F-mediated reprogramming, compared with Dox-treated *rtTA*-expressing WT MEFs (Figure 4K). Furthermore, overexpression of *PHF20* could reverse the Jmjd3-mediated inhibition of reprogramming (Figure 4L). The increased reprogramming efficiency in Tet-O-*PHF20* MEFs was not due to cellular proliferative activity, because there was no appreciable difference in cell growth between WT and Tet-O-*PHF2*0 MEFs, with or without Dox treatment (Figures S4J). Instead, Dox-induced expression of *PHF20* markedly blocked

NIH-PA Author Manuscript

NIH-PA Author Manuscript

NIH-PA Author Manuscript

downregulation of *Oct4*, *Sox2* and *Nanog* in iPSCs and thus their differentiation after LIF withdrawal (Figures S4K and S4L). Nonetheless, *PHF20* overexpression could not substitute for any of the 4F (Figure S4M). These results indicate as essential requirement for PHF20 in somatic cell reprogramming.

## Jmjd3 Interacts with PHF20 and Mediates its Proteasomal Degradation

To dissect the molecular mechanisms by which Jmjd3 and PHF20 reciprocally control reprogramming, we first showed their localization in the nucleus by immunofluorescent staining and fractionation experiment of ESCs and iPSCs (Figures S5A-S5B). Coimmunoprecipitation (co-IP) and western blot analyses of 293T cells transfected with Flag-*PHF20* and HA-*Jmjd3* revealed that Jmjd3 interacted with PHF20 (Figure 5A). Similar results were obtained with WT MEFs but not with *PHF20*-deficient MEFs (Figure 5B), suggesting that Jmjd3 interacts with PHF20 under physiological conditions. We then performed domain-mapping experiments with *Jmjd3-N* (1-450 aa), *Jmjd3-M* (400-1200 aa) and *Jmjd3-C* (1201-1683 aa), showing that the *Jmjd3-N* and *Jmjd3-C* constructs, but not *Jmjd3-M*, interacted with PHF20 (Figure 5C). Similarly, the N-terminal region (1-332 aa containing a DNA binding domain), but not the C-terminal region, of PHF20 interacted with Jmjd3 (Figure 5D and Figure S5C). Further experiments showed that Jmjd3, but not Utx or Uty, interacted with PHF20 (Figure S5D), suggesting that Jmjd3 specifically interacts with PHF20 via their functional domains.

What are the functional consequences of the Jmjd3-PHF20 interaction? To address this question, we transfected 293T cells with a fixed amount of Flag-*PHF20* together with increasing amounts of HA-*Jmjd3*, and found that the amounts of PHF20 protein decreased with increasing expression of Jmjd3 protein (Figure S5E). Similarly, the amounts of endogenous PHF20 protein were decreased in 293T cells transfected with increasing amounts of *Jmjd3* cDNA (Figure 5E). Furthermore, the amount of endogenous PHF20 protein in *Jmjd3*-deficient MEFs was much higher than in WT MEFs, while ectopic expression of *Jmjd3* cDNA in *Jmjd3*-deficient MEFs reduced the amount of PHF20 protein to a level similar to that in WT MEFs (Figure 5F). It, therefore, appears that Jmjd3 negatively regulates PHF20 protein by targeting it for degradation.

## Trim26 is an E3 Ubiquitin Ligase Required for PHF20 Ubiquitination and Degradation

To determine how Jmjd3 causes the degradation of PHF20, we first tested whether this protein is ubiquitinated in 293T cells expressing WT, K48 or K63 ubiquitin. PHF20 strongly underwent K48-linked ubiquitination, with little or no K63-linked ubiquitination, and such an ubiquitination was observed only when *Jmjd3* and *PHF20* were coexpressed (Figure 6A), suggesting that Jmjd3 specifically targets PHF20 for K48-linked polyubiquitination.

Since Jmjd3 is not an E3 ubiquitin ligase, we reasoned that Jmjd3 might function as an adaptor to recruit an E3 ubiquitin ligase to PHF20 for ubiquitination. To test this prediction, we designed a screen using 293T cells transfected with *Jmjd3* expression vector and a lentivirus-based shRNA sublibrary against human E3 ubiquitin ligases, as previously described (Cui et al., 2012). In an initial screening of about 600 shRNAs, we identified an E3 ubiqtuitin ligase (*Trim26*)-specific shRNA that was associated with increased PHF20 protein amounts, relative to results with control shRNA (Figures S6A and S6B). To substantiate this finding, we selected two shRNAs for human *Trim26* and three for murine *Trim26*, with 60-90% knockdown efficiency (Figures S6C and S6D). Knockdown of endogenous *Trim26* by shRNAs markedly abrogated Jmjd3-mediated ubiquitination of PHF20 in 293T cells (Figure 6B), with similar results obtained when either *Jmjd3* or *Trim26* was knocked down in $PHF20^{+/+}$ MEFs (Figure S6E). Consistent with these results, we found that knockdown of *Trim26* increased reprogramming efficiency in *PHF20* WT MEFs,

NIH-PA Author Manuscript

NIH-PA Author Manuscript

NIH-PA Author Manuscript

but not in *PHF20*-deficient MEFs (Figure 6C). Furthermore, knockdown of *Trim26* reversed Jmjd3-mediated inhibition of reprogramming (Figures S6F), while overexpression of *Trim26* inhibited reprogramming efficiency enhanced by *Jmjd3* knockdown (Figure S6G).

Because Trim26 and Jmjd3 could act in concert to modulate reprogramming through targeting PHF20 for ubiquitination and degradation, we next determined their expression patterns during reprogramming, and found that Trim26 was decreased while Jmjd3 was increased (Figure 6D). As expected, PHF20 expression gradually increased, but PHF20 protein in *Jmjd3*$^{-/-}$ MEFs was significantly higher than that in WT cells during reprogramming (Figures 6D and S6H). Although treatment with the protease inhibitor MG132 blocked protein degradation even when both *Trim26* and *Jmjd3* were overexpressed (Figure S6I), it was non-specific and caused cell death. Thus, we did not observe any iPSC colony formation after MG132 treatment (Figure S6J).

We then asked whether ectopic expression of *Trim26* would promote PHF20 ubiquitination and degradation. Indeed, coexpression of *Trim26* and *Jmjd3* led to a remarkable increase in K48-linked ubiquitination and degradation of PHF20, compared with *Trim26* or *Jmjd3* alone (Figure 6E). To determine whether Trim26 interacts with Jmjd3 or PHF20, we performed immunoprecipitation experiments using cells that expressed *Jmjd3*, *Trim26* alone or *PHF20* and *Trim26* together. Although Trim26 interacted with Jmjd3 but not PHF20 (Figure 6F), we detected both Jmjd3 and PHF20 in the anti-Flag-Trim26 immunoprecipitants of the cells that expressed *Jmjd3*, *PHF20* and *Trim26* (Figure 6F), suggesting that Jmjd3 is an adaptor protein that recruits Trim26 to PHF20. To determine which domain of Jmjd3 is responsible for recruiting Trim26 to PHF20, we transfected 293T cells with *Jmjd3*-N, *Jmjd3*-M or *Jmjd3*-C together with *Trim26*. Immunoprecipitation and western blot experiments revealed that the N-terminus of Jmjd3 (Jmjd3-N), but not Jmjd3-M and Jmjd3-C, was capable of binding to Trim26 (Figure 6G). To identify the domain of Jmjd3 that is required for Trim26-mediated ubiquitination of PHF20, we transfected 293T cells with Flag-*PHF20* together with HA-tagged *Jmjd3-N*, *Jmjd3-M*, *Jmjd3-C*, *Jmjd3-ΔJmjC*, *Jmjd3*-H1390A, or full-length *Jmjd3*. After immunoprecipitation with anti-Flag, we assessed K48-linked ubiquitination of PHF20, observing that none of the *Jmjd3-N*, *Jmjd3-M* and *Jmjd3-C* constructs were sufficient to cause PHF20 ubiquitination (Figure 6H). By contrast, like full-length *Jmjd3*, *Jmjd3-ΔJmjC* and *Jmjd3-H1390A* were able to mediate PHF20 ubiquitination (Figure 6H), consistent with results showing that *Jmjd3-ΔJmj*C and *Jmjd3-H1390A* could still inhibit iPSC reprogramming in *Jmjd3*-deficient MEFs (Figure 3F). These results suggest that the N-terminus of Jmjd3 (Jmjd3-N) can interact with Trim26, but is not sufficient to cause PHF20 ubiquitination. Jmjd3 containing the first 1200 aa or a point mutation (Jmjd3-ΔJmjC or Jmjd3-H1390A) is necessary and sufficient to target PHF20 for ubiquitination by recruiting the E3 ligase Trim26.

## PHF20 Is Required for Endogenous *Oct4* Expression and Interacts with Wdr5 During Reprogramming

Since PHF20 is essential for reprogramming in both WT and *Jmjd3*-deficient MEFs, we reasoned that it might be required for the reactivation of endogenous key genes such as *Oct4* and other markers of ESCs. To test this prediction, we examined the effects of PHF20 loss on the activation of 11 ESC markers during Tet-O-4F reprogramming, using WT and *PHF20*$^{-/-}$ MEFs in the presence of Dox for the first 10 days (and then withdrawal). Real-time PCR analysis on day 14 revealed that expression of *Oct4*, *Sox2*, *Nanog*, *Dnmt3l*, *Esg1*, *Eras*, *Rex1*, and *Cripto* could not be activated or substantially reduced in *PHF20*-deficient MEFs, but were highly activated in WT MEFs. By contrast, *Stat3, Grb2 and β-catenin* were activated normally in both WT and *PHF20*-deficient cells (Figure 7A). Notably, *Sox2* and *Nanog* could be reactivated when Dox was retained during reprogramming (Figure S7A). Overexpression of *Oct4* or even 4F could not rescue the incompletely reprogrammed

NIH-PA Author Manuscript

NIH-PA Author Manuscript

NIH-PA Author Manuscript

phenotype of *PHF20*-deficient MEFs after reprogramming (Figure S7B), suggesting that PHF20 is an upstream factor that controls many key reprogramming and pluripotency factors.

Because reactivation of endogenous *Oct4* is essential for the generation of completely reprogrammed iPSCs (Ang et al., 2011), we next determined whether PHF20 could directly bind to the *Oct4* promoter *in vivo*. ChIP-PCR assay revealed that PHF20 was strongly bound to this promoter in WT ESCs and iPSCs, but not in *PHF20*-deficient (differentiated) ESCs and (incompletely reprogrammed) iPSCs (Figures 7B and 7C). PHF20 was unable to bind to the promoter regions of *Cripto*, *Dnmt3l*, *Esg1*, *Eras*, *Nonog*, *Rex1* or *Sox2* (Figure S7C). Furthermore, the binding of PHF20 to the *Oct4* promoter increased gradually over the course of reprogramming (Figure 7D). To further determine whether overexpression of *PHF20* could promote expression of endogenous *Oct4*, we treated both WT and Tet-O-*PHF20* MEFs expressing *rtTA* with Dox during 4F-mediated reprogramming. The expression level of *Oct4* was markedly increased in Dox-treated Tet-O-*PHF20* MEFs, compared with Dox-treated *rtTA*-expressing WT MEFs (Figure 7E), suggesting that PHF20 promotes endogenous *Oct4* gene expression during reprogramming.

Because the DNA methylation status of the *Oct4* promoter serves as an important marker of fully reprogrammed iPSCs (Stadtfeld and Hochedlinger, 2010), we undertook bisulfate sequencing analysis of ESCs and iPSCs generated from WT MEFs, which showed robust DNA demethylation in the *Oct4* promoter regions. By contrast, incompletely reprogrammed iPSC colonies from *PHF20*-deficient MEFs retained their DNA methylation pattern (Figure 7F). More importantly, we showed that ectopic expression of PHF20 could rescue the incompletely reprogrammed state of *PHF20*-deficient iPSCs and the status of the *Oct4* promoter demethylation, similar to results for WT iPSCs (Figure 7F).

PHF20 is a component of mixed-lineage leukemia (MLL) H3K34 methyltransferase complexes with the core components MLL, ASH2L, WDR5 and RBBP5, as well as a component of the H4K16 acetyltransferase MOF (male-absent on the first, also called MYST1, KAT8) complex (Cai et al., 2010; Dou et al., 2005; Wysocka et al., 2005). Importantly, Wdr5 is also a key component shared by MLL H3K4 methyltransferase and the H4K16 acetyltransferase MOF (Cai et al., 2010; Dou et al., 2005; Wysocka et al., 2005). However, it is not known whether PHF20 interacts with Wdr5 or other components of these two complexes. Because PHF20 is upregulated and binds to the *Oct4* promoter during reprogramming, we predicted that PHF20 might interact with Wdr5 to promote endogenous *Oct4* expression during reprogramming. To test this possibility, we transfected 293T cells with *PHF20* together with *Wdr5*, *MLL3*, *Dpy-30*, *Ash2l* or *RbBP5*, all core components of the H3K4 methyltransferase complex (Trievel and Shilatifard, 2009). PHF20 interacted with Wdr5, but not with other proteins tested (Figures 7G and S7D). Endogenous interactions between PHF20 and Wdr5 or RbBP5 (but not Ash2L) were observed in iPSCs (Figure 7H). ChIP-seq analysis of ESCs and iPSCs confirmed that both PHF20 and Wdr5 were bound to the *Oct4* promoter (Figure S7E). Among 6209 genes bound by PHF20 and 7774 genes by Wdr5, approximately 2348 genes were co-occupied by PHF20 and Wdr5 in ESCs (Figure S7F and Table S3). To determine the PHF20 and Wdr5 binding distribution relative to gene structure (i.e. 5′ distal, 5′ proximal, 5′ UTR, Coding, intron, 3′ UTR, 3′ proximal and 3′ distal regions), we found that the majority of PHF20 and Wdr5 binding sites were mapped to gene body (coding and intron regions) and 5′ proximal region in ESCs (Figure S7G). The distribution of PHF20 was more pronounced toward 5′ end of genes with 9.7% peaks at 5′ proximal region, compared to 2.8% at 3′ proximal region (Figure S7G). Consistent with this, we found that both PHF20 and Wdr5 binding peaks centered on TSS within a 7 kb region (from -2 to +5 kb) (Figure S7H). To determine functional relevance of target genes bound by PHF20 or by PHF20 and Wdr5, we performed gene ontology (GO) analysis and

NIH-PA Author Manuscript

NIH-PA Author Manuscript

NIH-PA Author Manuscript

found that binding targets were enriched for genes involved in cell and organ developmental process, embryonic development, and cell differentiation (Figure S7I).

To determine whether PHF20 interacts with MOF, we performed co-immunoprecipitation with anti-PHF20, and found that PHF20 interacted with endogenous MOF in iPSCs (Figure 7H), consistent with the results of a recent report showing that H3K4 methylation is closely associated with H4K16 acetylation (Wang et al., 2009). Thus, PHF20 interacts with Wdr5 and MOF to bring the H3K4 methyltransferase complex and H4K16 aceyltransferase MOF complex together. To understand how the loss of PHF20 results in failure to reactivate endogenous *Oct4* expression, we tested the possibility that PHF20 might affect the ability of Wdr5, RbBP5 and MOF to bind to the *Oct4* promoter region. In ChIP-PCR experiments with WT and *PHF20*-deficient cells, Wdr5 failed to bind to the *Oct4* promoter in PHF20-deficient cells, but bound strongly to the *Oct4* promoter in WT cells (Figure 7I). Similarly, the ability of RbBP5 and MOF to bind to the *Oct4* promoter was markedly reduced in *PHF20*-deficient cells. Consistent with these results, ChIP-qPCR experiments revealed a sharp reduction in H3K4 trimethylation in the *Oct4* promoter, while H4K16 acetylation was also affected but to a lesser extent (Figure 7J). Taken together, these results suggest that binding of PHF20 to the *Oct4* promoter may be required for recruiting H3K4 methyltransferase complex and perhaps H4K16 acetlytransferase complex to bind to the same promoter through the interaction with Wdr5 and MOF, leading to reactivation of endogenous *Oct4* expression during reprogramming.

## Discussion

Using a shRNA knockdown screen in Tet-O-4F MEFs, we identified a number of histone-modifying proteins that are required for the reprogramming of somatic cells to iPSCs, but only one, Jmjd3, functions as a negative regulator of this process. Given the sequential multistep nature of iPSC generation (Plath and Lowry, 2011), it is not surprising that negative regulators of reprogramming exist. Indeed, DOT1L was recently shown to negatively control Nanog and LIN28 expression, posing an unexpected barrier to efficient reprogramming (Onder et al., 2012). Until the full spectrum of such regulators is delineated and their mechanisms of action deciphered, it will be difficult to revise current approaches to iPSC generation with any degree of confidence.

Jmjd3 plays a critical role in the upregulation of *Ink4a/Arf* by modulating the levels of H3K27 trimethylation in the promoter (Agger et al., 2009; Barradas et al., 2009). These effects on the expression of *Ink4a/Arf* and *p21*, in turn, induce senescence and inhibit reprogramming (Hong et al., 2009; Kawamura et al., 2009; Li et al., 2009; Marion et al., 2009; Utikal et al., 2009), consistent with our demonstration that *Jmjd3* ablation reduces cell senescence and promotes reprogramming of *Jmjd3*-deficient MEFs. However, we provide several lines of evidence indicating that Jmjd3 can regulate reprogramming through a previously unrecognized, histone demethylase activity-independent pathway. First, the combined knockdown of *Jmjd3* with *Ink4a* or *p21* resulted in significantly more iPSC colonies than did knockdown of any single gene alone. Second, although ectopic expression of full-length *Jmjd3* in *Jmjd3*-deficient MEFs restored *Ink4a/Arf* expression and strongly inhibited the efficiency of reprogramming, the *Jmjd3* mutants *Jmjd3-ΔJmjC* and *Jmjd3-H1390A,* defined by their lack of H3K27me3 demethylase activity and inability to upregulate *Ink4a/Arf* expression, could still inhibit reprogramming in *Jmjd3*-deficient MEFs. We therefore propose that Jmjd3 exploits both demethylase activity-dependent and -independent mechanisms to regulate somatic cell reprogramming, with the latter having a predominant role.

NIH-PA Author Manuscript

NIH-PA Author Manuscript

NIH-PA Author Manuscript

An extensive search for target molecules that might be involved in a Jmjd3-mediated but demethylase activity-independent pathway led to the identification of PHF20. We provide evidence of a critical role for PHF20 expression in the maintenance of the pluripotent state. PHF20 was first identified as an antibody-reactive protein that is highly expressed in several types of cancer (Fischer et al., 2001; Wang et al., 2002). PHF20 has since been identified as a histone code reader that specifically recognizes the dimethylation of H3K4, H3K9, H4K20, and H4K79 (Adams-Cioaba et al., 2012; Kim et al., 2006). Recent studies show that it also regulates p53 protein at both the transcriptional and posttranscriptional levels in response to DNA damage (Li et al., 2012b; Park et al., 2012). Mice with PHF20 ablation die shortly after birth (Badeaux et al., 2012). Consistently, we failed to generate ESC lines from *PHF20* knockout mice. *PHF20* deficiency almost completely inhibits reprogramming of *PHF20*-deficient MEFs, suggesting an absolute requirement for this factor in iPSC reprogramming and generation of ESCs.

Jmjd3 has been shown to play an important role in T cell-lineage commitment by interacting with T-bet and Brg-1 in a demethylase activity-independent manner (Miller et al., 2010). Here we show that Jmjd3 interacts with PHF20, targeting it for ubiquitination and proteasomal degradation. Although both the N- and C-terminal regions of Jmjd3 protein can bind to the N-terminus of PHF20, Jmjd3 itself cannot ubiquitinate PHF20 in a K48-linkage. Instead, it recruits an E3 ligase, Trim26, to PHF20 for K48-linked polyubiquitination. Indeed, knockdown of *Trim26* abolishes PHF20 ubiquitination and degradation, thus enhancing iPSC reprogramming. Further experiments demonstrated that like full-length Jmjd3, certain Jmjd3 mutants (Jmjd3-ΔJmjC and Jmjd3-H1390A), but not Jmjd3-N, Jmjd3-M, or Jmjd3-C, target PHF20 for ubiquitination. These results emphasize the importance of Jmjd3-Trim26 mediated ubiquitination in the negative regulation of reprogramming.

Fully reprogrammed iPSCs are accompanied by changes in distinct DNA methylation patterns associated with reactivation of endogenous Oct4 and several other ESC marker genes (Plath and Lowry, 2011; Stadtfeld and Hochedlinger, 2010). How, then, does PHF20 deficiency lead to failure to reactivate these endogenous marker genes, thus imposing a major barrier to successful reprogramming? A recent study shows that exogenous Oct4 together with other key reprogramming factors first induce *Wdr5* expression in MEFs, which in turn forms a Wdr5-Oct4 complex that binds to the *Oct4* promoter, leading to reactivation of endogenous *Oct4* expression (Ang et al., 2011). To directly link PHF20 to Oct4 expression, we show that PHF20 not only binds to the *Oct4* promoter region, but also specifically interacts with Wdr5 and MOF. A recent study shows that MOF is required for ESC self-renewal and function, and regulates Nanog expression (Li et al., 2012a). Deletion of PHF20 reduces the ability of Wdr5 and MOF to bind to the *Oct4* promoter, suggesting a critical requirement for this protein in reactivation of endogenous *Oct4* expression and hence for successful generation of fully reprogrammed iPSCs. Consistent with this notion, our results further demonstrated that *PHF20* deficiency results in failure to reactivate expression of many endogenous ESC maker genes during reprogramming, suggesting that PHF20 affects expression of many key ESC genes directly or indirectly. ChIP-PCR and ChIP-seq analyses show that PHF20 and Wdr5 bind to the *Oct4* promoter, but not to the promoter regions of *Sox2, Nanog*, *Dnmt3l*, *Esg1*, *Eras*, *Rex1* and *Cripto*. In addition, ChIP-seq analysis revealed that both PHF20 and Wdr5 bind to several key epigenetic factor genes, including *Baf155*, *Brg-1* and *Sall4*. Hence, these findings explain why the incompletely reprogrammed phenotype of *PHF20*-deficient MEFs cannot be rescued by overexpression of *Oct4* or 4F (OSKM), and further suggest that PHF20 functions as a upstream regulator that control *Oct4* and many other critical ESC marker genes, thus providing a mechanistic link between Jmjd3-mediated PHF20 degradation and deficient reprogramming.

NIH-PA Author Manuscript

NIH-PA Author Manuscript

NIH-PA Author Manuscript

On the basis of these findings, we propose a working model to explain how the Jmjd3-PHF20 axis regulates iPSC reprogramming. Increased expression of Jmjd3 due to 4F-mediated reprogramming in WT MEFs initiates at least two distinct pathways (Figure 7K): 1) Jmjd3upregulates *Ink4a/Arf* and *p21* by modulating H3K4 and H3K27 methylation through itsH3K27me2/3 demethylase activity. Increased amounts of Ink4a, Arf and p21 induce cell senescence or apoptosis and reduce cell proliferation, thus decreasing the efficiency and kinetics of reprogramming; 2) Jmjd3 protein also targets PHF20 for ubiquitination and degradation by recruiting an E3 ligase, Trim26, in a H3K27 demethylase activity-independent manner. The resultant decrease in PHF20 protein leads to the loss or negligible expression of endogenousOct4, thereby greatly reducing reprogramming efficiency. We conclude that the demethylase activity-dependent and -independent pathways used by Jmjd3 act in concert to potently restrain the kinetics and efficiency of reprogramming. The observations that Jmjd3 loss reduces cells senescence and apoptosis and increases cell proliferation, and that increased amounts of PHF20lead to reactivation of endogenous *Oct4* expression, suggest means to enhance the outcome of somatic cell reprogramming overall.

## Experimental Procedures

### Mice

Tet-O-*Sox2* and -*Klf4* transgenic mice were generated and crossed with Rosa-*rtTA*, Tet-O-*Oct4* (from the Jackson Laboratories) and Tet-O-*Myc* transgenic mice. Tet-O-4F MEFs that express *rtTA* and Tet-O-*Oct4*, *Sox2*, *Klf4* and *Myc* were established and used for reprogramming. Tet-O-*PHF20* mice were generated as Tet-O-*Sox2* and -*Klf4* transgenic mice. *Jmjd3* was targeted deletion of exon 15-21 using a Cre-LoxP system. *Jmjd3* was globally deleted by crossing $Jmjd3^{f/f}$ mice with *Hprt*-Cre mice (Jackson Laboratories).

### Generation of iPSCs from MEFs and Tet-O-4F MEFs

Mouse iPSCs were generated from MEFs, as previously described (Takahashi et al., 2007a) with some minor modifications. Tet-O-4F MEFs were used to generate iPSCs by treating MEFs with Dox in mESC medium. The efficiency of iPSC formation as calculated based on the number of $AP^+$ iPSC colonies and the initial cell number of seeded MEFs. Human iPSCs were generated as previously described (Park et al., 2008). Lentiviral particles were generated and concentrated, as previously described (Peng et al., 2005).

### Screening for Epigenetic Factors that Modulate Reprogramming Efficiency

Tet-O-4F transgenic MEF cells (M2-11) were transduced with lentiviras-based shRNAs specific for 15 epigenetic factors and then reseeded on irradiated feeder cells at the desired density. The next day, mESC medium containing 2 μg/ml Dox was added and replenished every day. The colonies were stained for AP activity on Days 12-14.

### Co-IP, ChIP-PCR and ChIP seq Analysis

The cells were lysed in RIPA buffer, and analyzed, as previously described (Cui et al., 2010). ChIP assay was performed with Imprint Ultra Chromatin Immunoprecipitation kit (Sigma). ChIP-Seq libraries were prepared, sequenced and analyzed. See the Extended Experimental Procedures for details.

### Accession Numbers

The ChIP-seq data are available at the Gene Expression Omnibus under the accession number GSE43247.

NIH-PA Author Manuscript

NIH-PA Author Manuscript

NIH-PA Author Manuscript

## Supplementary Material

Refer to Web version on PubMed Central for supplementary material.

## Acknowledgments

We would like to thank Drs Yi Li at Baylor College of Medicine for providing Tet-O-Myc transgenic mice, Mark Bedford at M.D. Anderson Cancer Center for PHF20 knockout mice, Dan Liu at Baylor College of Medicine for assistance for shRNA screening, and Paul Webb for assistance in ChIP-seq experiments. We would also like to thank John Gilbert and Adebusola A. Ajibade for their critical reading of this manuscript. This work was in part supported by grants from National Cancer Institute, NIH (P01CA094237, R01CA09327, R01CA101795, R01CA116408, R01CA121191 and R01 DA030338) and Cancer Prevention and Research Institute of Texas (RP121048) to R.F.W and The Methodist Hospital Research Institute.

## References

Adams-Cioaba MA, Li Z, Tempel W, Guo Y, Bian C, Li Y, Lam R, Min J. Crystal structures of the Tudor domains of human PHF20 reveal novel structural variations on the Royal Family of proteins. FEBS Lett. 2012; 586:859–865. [PubMed: 22449972]

Agger K, Cloos PA, Christensen J, Pasini D, Rose S, Rappsilber J, Issaeva I, Canaani E, Salcini AE, Helin K. UTX and JMJD3 are histone H3K27 demethylases involved in HOX gene regulation and development. Nature. 2007; 449:731–734. [PubMed: 17713478]

Agger K, Cloos PA, Rudkjaer L, Williams K, Andersen G, Christensen J, Helin K. The H3K27me3 demethylase JMJD3 contributes to the activation of the INK4A-ARF locus in response to oncogene- and stress-induced senescence. Genes Dev. 2009; 23:1171–1176. [PubMed: 19451217]

Ang YS, Tsai SY, Lee DF, Monk J, Su J, Ratnakumar K, Ding J, Ge Y, Darr H, Chang B, et al. Wdr5 mediates self-renewal and reprogramming via the embryonic stem cell core transcriptional network. Cell. 2011; 145:183–197. [PubMed: 21477851]

Badeaux AI, Yang Y, Cardenas K, Vemulapalli V, Chen K, Kusewitt D, Richie E, Li W, Bedford MT. Loss of the methyl lysine effector protein PHF20 impacts the expression of genes regulated by the lysine acetyltransferase MOF. J Biol Chem. 2012; 287:429–437. [PubMed: 22072714]

Barradas M, Anderton E, Acosta JC, Li S, Banito A, Rodriguez-Niedenfuhr M, Maertens G, Banck M, Zhou MM, Walsh MJ, et al. Histone demethylase JMJD3 contributes to epigenetic control of INK4a/ARF by oncogenic RAS. Genes Dev. 2009; 23:1177–1182. [PubMed: 19451218]

Cai Y, Jin J, Swanson SK, Cole MD, Choi SH, Florens L, Washburn MP, Conaway JW, Conaway RC. Subunit composition and substrate specificity of a MOF-containing histone acetyltransferase distinct from the male-specific lethal (MSL) complex. J Biol Chem. 2010; 285:4268–4272. [PubMed: 20018852]

Cui J, Li Y, Zhu L, Liu D, Songyang Z, Wang HY, Wang RF. NLRP4 negatively regulates type I interferon signaling by targeting the kinase TBK1 for degradation via the ubiquitin ligase DTX4. Nat Immunol. 2012; 13:387–395. [PubMed: 22388039]

Cui J, Zhu L, Xia X, Wang HY, Legras X, Hong J, Ji J, Shen P, Zheng S, Chen ZJ, et al. NLRC5 negatively regulates the NF-kappaB and type I interferon signaling pathways. Cell. 2010; 141:483–496. [PubMed: 20434986]

Dou Y, Milne TA, Tackett AJ, Smith ER, Fukuda A, Wysocka J, Allis CD, Chait BT, Hess JL, Roeder RG. Physical association and coordinate function of the H3 K4 methyltransferase MLL1 and the H4 K16 acetyltransferase MOF. Cell. 2005; 121:873–885. [PubMed: 15960975]

Fischer U, Struss AK, Hemmer D, Pallasch CP, Steudel WI, Meese E. Glioma-expressed antigen 2 (GLEA2): a novel protein that can elicit immune responses in glioblastoma patients and some controls. Clin Exp Immunol. 2001; 126:206–213. [PubMed: 11703362]

Gaspar-Maia A, Alajem A, Meshorer E, Ramalho-Santos M. Open chromatin in pluripotency and reprogramming. Nat Rev Mol Cell Biol. 2011; 12:36–47. [PubMed: 21179060]

Hanna J, Saha K, Pando B, van Zon J, Lengner CJ, Creyghton MP, van Oudenaarden A, Jaenisch R. Direct cell reprogramming is a stochastic process amenable to acceleration. Nature. 2009; 462:595–601. [PubMed: 19898493]

NIH-PA Author Manuscript

NIH-PA Author Manuscript

NIH-PA Author Manuscript

Hemberger M, Dean W, Reik W. Epigenetic dynamics of stem cells and cell lineage commitment: digging Waddington's canal. Nat Rev Mol Cell Biol. 2009; 10:526–537. [PubMed: 19603040]

Hong H, Takahashi K, Ichisaka T, Aoi T, Kanagawa O, Nakagawa M, Okita K, Yamanaka S. Suppression of induced pluripotent stem cell generation by the p53-p21 pathway. Nature. 2009; 460:1132–1135. [PubMed: 19668191]

Kawamura T, Suzuki J, Wang YV, Menendez S, Morera LB, Raya A, Wahl GM, Izpisua Belmonte JC. Linking the p53 tumour suppressor pathway to somatic cell reprogramming. Nature. 2009; 460:1140–1144. [PubMed: 19668186]

Kim J, Daniel J, Espejo A, Lake A, Krishna M, Xia L, Zhang Y, Bedford MT. Tudor, MBT and chromo domains gauge the degree of lysine methylation. EMBO Rep. 2006; 7:397–403. [PubMed: 16415788]

Koche RP, Smith ZD, Adli M, Gu H, Ku M, Gnirke A, Bernstein BE, Meissner A. Reprogramming factor expression initiates widespread targeted chromatin remodeling. Cell Stem Cell. 2011; 8:96–105. [PubMed: 21211784]

Lan F, Bayliss PE, Rinn JL, Whetstine JR, Wang JK, Chen S, Iwase S, Alpatov R, Issaeva I, Canaani E, et al. A histone H3 lysine 27 demethylase regulates animal posterior development. Nature. 2007; 449:689–694. [PubMed: 17851529]

Li H, Collado M, Villasante A, Strati K, Ortega S, Canamero M, Blasco MA, Serrano M. The Ink4/Arf locus is a barrier for iPS cell reprogramming. Nature. 2009; 460:1136–1139. [PubMed: 19668188]

Li R, Liang J, Ni S, Zhou T, Qing X, Li H, He W, Chen J, Li F, Zhuang Q, et al. A mesenchymal-to-epithelial transition initiates and is required for the nuclear reprogramming of mouse fibroblasts. Cell Stem Cell. 2010; 7:51–63. [PubMed: 20621050]

Li X, Li L, Pandey R, Byun JS, Gardner K, Qin Z, Dou Y. The histone acetyltransferase MOF is a key regulator of the embryonic stem cell core transcriptional network. Cell Stem Cell. 2012a; 11:163–178. [PubMed: 22862943]

Li Y, Park J, Piao L, Kong G, Kim Y, Park KA, Zhang T, Hong J, Hur GM, Seok JH, et al. PKB-mediated PHF20 phosphorylation on Ser291 is required for p53 function in DNA damage. Cell Signal. 2012b; 25:74–84. [PubMed: 22975685]

Mansour AA, Gafni O, Weinberger L, Zviran A, Ayyash M, Rais Y, Krupalnik V, Zerbib M, Amann-Zalcenstein D, Maza I, et al. The H3K27 demethylase Utx regulates somatic and germ cell epigenetic reprogramming. Nature. 2012; 488:409–413. [PubMed: 22801502]

Marion RM, Strati K, Li H, Murga M, Blanco R, Ortega S, Fernandez-Capetillo O, Serrano M, Blasco MA. A p53-mediated DNA damage response limits reprogramming to ensure iPS cell genomic integrity. Nature. 2009; 460:1149–1153. [PubMed: 19668189]

Miller SA, Mohn SE, Weinmann AS. Jmjd3 and UTX play a demethylase-independent role in chromatin remodeling to regulate T-box family member-dependent gene expression. Mol Cell. 2010; 40:594–605. [PubMed: 21095589]

Onder TT, Kara N, Cherry A, Sinha AU, Zhu N, Bernt KM, Cahan P, Marcarci BO, Unternaehrer J, Gupta PB, et al. Chromatin-modifying enzymes as modulators of reprogramming. Nature. 2012; 483:598–602. [PubMed: 22388813]

Park IH, Lerou PH, Zhao R, Huo H, Daley GQ. Generation of human-induced pluripotent stem cells. Nat Protoc. 2008; 3:1180–1186. [PubMed: 18600223]

Park S, Kim D, Dan HC, Chen H, Testa JR, Cheng JQ. Identification of Akt Interaction Protein PHF20/TZP That Transcriptionally Regulates p53. J Biol Chem. 2012; 287:11151–11163. [PubMed: 22334668]

Peng G, Guo Z, Kiniwa Y, Voo KS, Peng W, Fu T, Wang DY, Li Y, Wang HY, Wang RF. Toll-like receptor 8 mediated-reversal of CD4+ regulatory T cell function. Science. 2005; 309:1380–1384. [PubMed: 16123302]

Plath K, Lowry WE. Progress in understanding reprogramming to the induced pluripotent state. Nat Rev Genet. 2011; 12:253–265. [PubMed: 21415849]

Robinton DA, Daley GQ. The promise of induced pluripotent stem cells in research and therapy. Nature. 2012; 481:295–305. [PubMed: 22258608]

Stadtfeld M, Hochedlinger K. Induced pluripotency: history, mechanisms, and applications. Genes Dev. 2010; 24:2239–2263. [PubMed: 20952534]

NIH-PA Author Manuscript

NIH-PA Author Manuscript

NIH-PA Author Manuscript

Takahashi K, Okita K, Nakagawa M, Yamanaka S. Induction of pluripotent stem cells from fibroblast cultures. Nat Protoc. 2007a; 2:3081–3089. [PubMed: 18079707]

Takahashi K, Tanabe K, Ohnuki M, Narita M, Ichisaka T, Tomoda K, Yamanaka S. Induction of pluripotent stem cells from adult human fibroblasts by defined factors. Cell. 2007b; 131:861–872. [PubMed: 18035408]

Takahashi K, Yamanaka S. Induction of pluripotent stem cells from mouse embryonic and adult fibroblast cultures by defined factors. Cell. 2006; 126:663–676. [PubMed: 16904174]

Trievel RC, Shilatifard A. WDR5, a complexed protein. Nat Struct Mol Biol. 2009; 16:678–680. [PubMed: 19578375]

Utikal J, Polo JM, Stadtfeld M, Maherali N, Kulalert W, Walsh RM, Khalil A, Rheinwald JG, Hochedlinger K. Immortalization eliminates a roadblock during cellular reprogramming into iPS cells. Nature. 2009; 460:1145–1148. [PubMed: 19668190]

Wang T, Chen K, Zeng X, Yang J, Wu Y, Shi X, Qin B, Zeng L, Esteban MA, Pan G, et al. The histone demethylases Jhdm1a/1b enhance somatic cell reprogramming in a vitamin-C-dependent manner. Cell Stem Cell. 2011; 9:575–587. [PubMed: 22100412]

Wang Y, Han KJ, Pang XW, Vaughan HA, Qu W, Dong XY, Peng JR, Zhao HT, Rui JA, Leng XS, et al. Large scale identification of human hepatocellular carcinoma-associated antigens by autoantibodies. J Immunol. 2002; 169:1102–1109. [PubMed: 12097419]

Wang Z, Zang C, Cui K, Schones DE, Barski A, Peng W, Zhao K. Genome-wide mapping of HATs and HDACs reveals distinct functions in active and inactive genes. Cell. 2009; 138:1019–1031. [PubMed: 19698979]

Wysocka J, Swigut T, Milne TA, Dou Y, Zhang X, Burlingame AL, Roeder RG, Brivanlou AH, Allis CD. WDR5 associates with histone H3 methylated at K4 and is essential for H3 K4 methylation and vertebrate development. Cell. 2005; 121:859–872. [PubMed: 15960974]

Yu J, Vodyanik MA, Smuga-Otto K, Antosiewicz-Bourget J, Frane JL, Tian S, Nie J, Jonsdottir GA, Ruotti V, Stewart R, et al. Induced pluripotent stem cell lines derived from human somatic cells. Science. 2007; 318:1917–1920. [PubMed: 18029452]

NIH-PA Author Manuscript

NIH-PA Author Manuscript

NIH-PA Author Manuscript

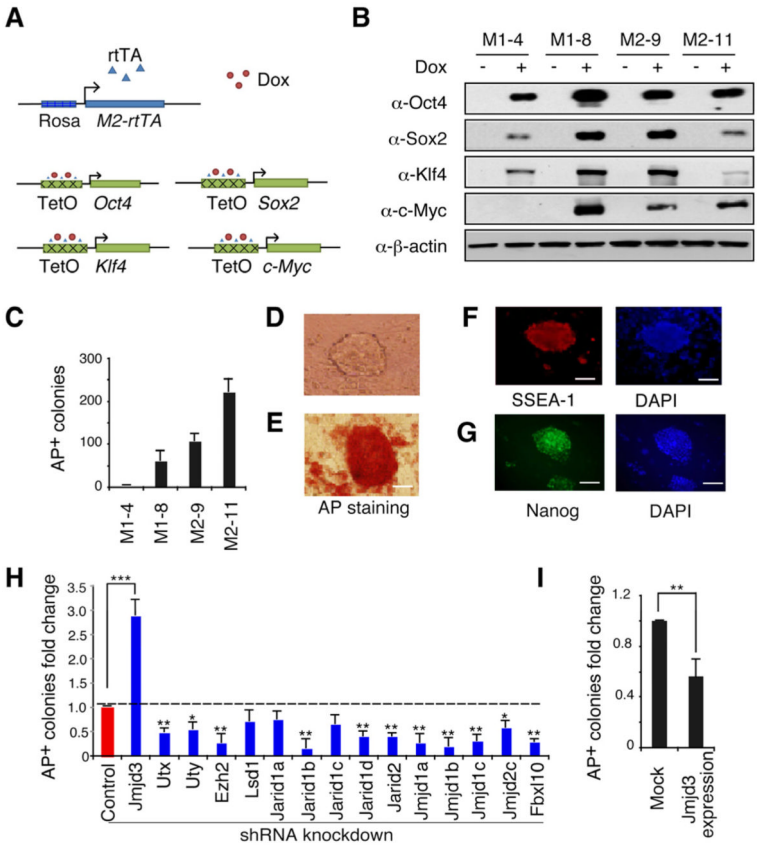


**Figure 1. Identification of Jmjd3 and Other Key Epigenetic Factors that Regulate Reprogramming**

(A) Outline of generation of transgenic mice expressing *rtTA*, together with *Oct4 (O)*, *Sox2 (S)*, *Klf4 (K)* and *Myc (M)* (OSKM, 4F) under control of a tetracycline-on promoter (Tet-O). (B) Western blot analysis of 4F expression in Tet-O MEFs treated with or without Dox. (C) Alkaline phosphatase (AP)-positive colonies were counted at day12 after Dox treatment. (D) Bright field images of an iPSC colony derived from Tet-O 4F MEFs. (E-G) Staining of representative iPSC colonies with antibodies against AP, stage-specific embryonic antigen 1 (SSEA1) and Nanog. Scale bars in panels D, E, F and G, 50μm (H) Fold changes in number of AP-positive colonies generated from Tet-O 4F MEFs transduced with specific shRNA, compared with control shRNA. AP-positive colonies were counted on day14 after Dox treatment. (I) Fold changes in number of AP-positive colonies generated from Tet-O 4F MEFs transduced with Jmjd3 expression or empty vector. Ectopic expression of *Jmjd3* inhibits reprogramming. The data in panels **H** and **I** are reported as the means ± SD with indicated significance (*p <0.05, **p < 0.01 ***p < 0.001 by Student's t test). See also Figure S1.

NIH-PA Author Manuscript

NIH-PA Author Manuscript

NIH-PA Author Manuscript

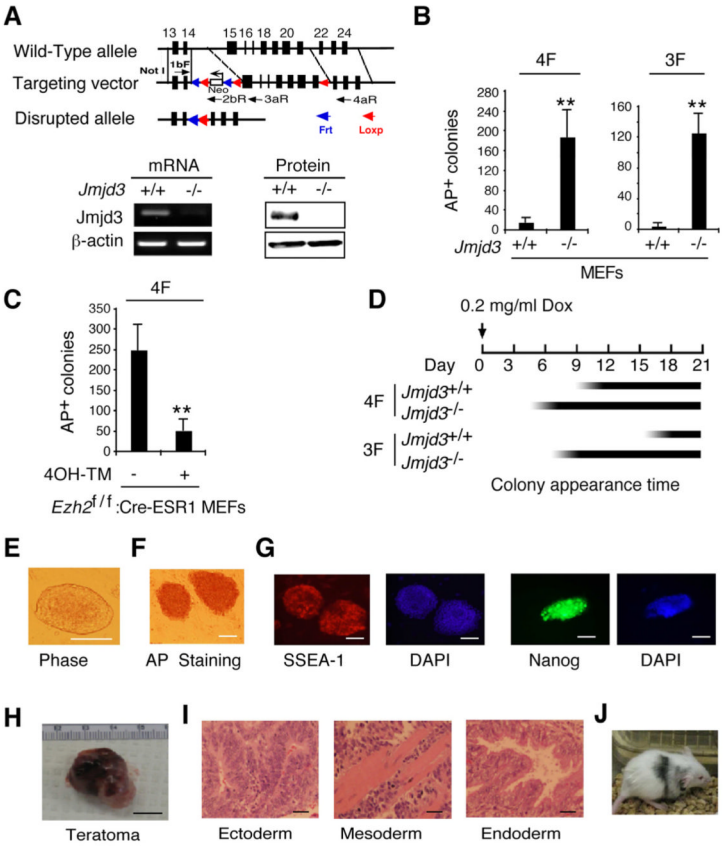


**Figure 2. Jmjd3 Ablation Enhances the Efficiency and Kinetics of Reprogramming**

(A) Establishment of *Jmjd3* knockout mice and *Jmjd3*-deficient MEFs. PCR and immunoblot (IB) analyses confirmed loss of *Jmjd3* expression in *Jmjd3*-deficient MEFs. (B) AP-positive colonies were counted on day 14 of 4F-mediated or on day 21 of 3F-mediated reprogramming of WT and *Jmjd3*-deficient MEF cells. (C) AP-positive colonies were counted on day 14 of 4F-mediated reprogramming after tamoxifen treatment of $Ezh2^{f/f}$ :Cre-ESR1 MEFs. (D) Schematic representation of the time of AP+ colony appearance during reprogramming. (E) Bright-field image of a representative iPSC colony generated from *Jmjd3*-deficient MEFs. (F and G) Staining of representative iPSC colonies with antibodies against AP, SSEA1 and Nanog. Scale bars, 50 μm. (H and I) Photomicrograph and HE (hematoxylin and eosin) staining of teratomas generated from immune-deficient mice harboring a *Jmjd3*-deficient iPSC clone. Three layers of teratoma (ectoderm, mesoderm and endoderm) are presented. Scale bars, 100 μm. (J) $Jmjd3^{-/-}$ MEF-derived iPSCs were pluripotent and contributed to chimeras after injection into BALB/C host blastocysts as indicated by coat color. The data in panels **B** and **C** are reported as means ± SD with indicated significance (*$p < 0.05$, **$p < 0.01$ by Student's t test).

NIH-PA Author Manuscript
NIH-PA Author Manuscript
NIH-PA Author Manuscript



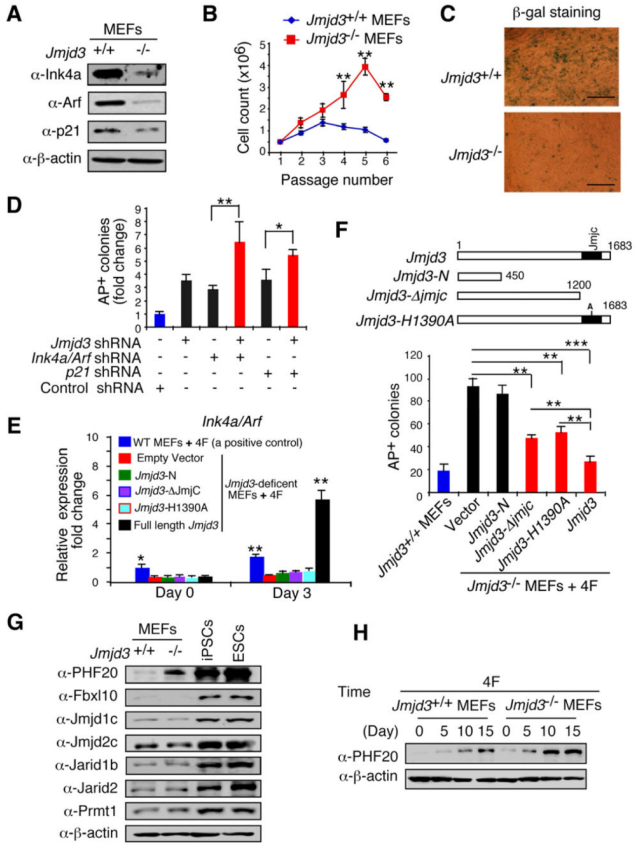


**Figure 3. Identification of Jmjd3 Targets Responsible for Enhanced Reprogramming**

(A) Western blot analysis of Ink4a, Arf and p21 in WT and *Jmjd3*-deficient MEFs at passage 4. (B) Growth of WT versus *Jmjd3*-deficient MEFs. (C) β-gal staining of WT versus *Jmjd3*-deficient MEFs at passage 4. (D) Number of AP-positive iPSC colonies counted on day 14 of 4F-mediated reprogramming of WT MEFs transduced with *Jmjd3*-, *Ink4a/Arf*-, *p21*-specific or control shRNAs. (E) *Jmjd3*-deficient MEFs transduced with lentiviruses expressing *Jmjd3* or its mutants together with 4F for 3 days. Expression of *Ink4a/Arf* was determined by real-time PCR analysis and was normalized by internal control beta-actin. (F) Number of AP-positive iPSC colonies counted on day 11 of 4F-mediated reprogramming of *Jmjd3*-deficient MEFs transduced with lentiviruses expressing *Jmjd3* or its mutants. (G) Western blot analysis of 7 epigenetic proteins in WT and *Jmjd3*-deficient MEFs, iPSCs and ES cells. (H) Western blot analysis of PHF20 expression in WT and *Jmjd3*-deficient MEFs during 4F-mediated reprogramming. The data in panels **B**, **D**-**F** are reported as means ± SD with indicated significance (*p < 0.05, **p < 0.01, ***p<0.001). See also Figures S2 and S3.

NIH-PA Author Manuscript

NIH-PA Author Manuscript

NIH-PA Author Manuscript

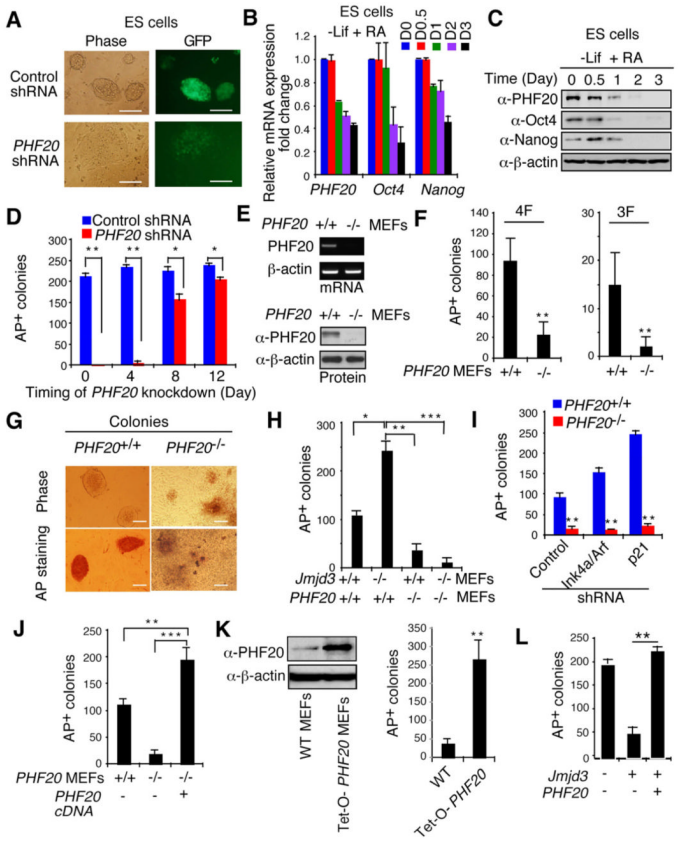


**Figure 4. PHF20 Is Essential for Maintenance and Reprogramming of iPSCs**

(A) Bright-field and GFP images of ESCs transduced with PHF20-specific or control shRNA. Scale bars, 50 μm. (B) Real-time PCR analysis of *PHF20*, *Oct4* and *Nanog* expression in ESCs treated with 1 mM RA and LIF withdrawal. (C) Western blot analysis of PHF20, Oct4 and Nanog expression after treatment of ESCs with 1 μM RA and LIF withdrawal. (D) Colony formation after PHF20 knockdown by *PHF20*-specific or a control lentivirus-based constitutive shRNA at different time points (i.e., day 0, 4, 8 or 12) during reprogramming of Tet-O-4F MEFs. AP-positive colonies were counted on day 14. (E) PCR and Western blot analyses of PHF20 expression in WT and *PHF20*-deficient MEFs. (F) AP-positive colony numbers were counted on day 14 of 3F- or 4F-mediated reprogramming of WT and *PHF20*-deficient MEFs. (G) Bright-field images and AP staining of iPSC-like colonies from WT and *PHF20*-deficient MEFs. Scale bars, 50 μm. (H) Number of AP-positive colonies counted on day 14 of 4F-mediated reprogramming of WT and *PHF20* single, or *Jmjd3* and *PHF20*-double KO MEFs. (I) Number of AP-positive colonies on day 14 of 4F-mediated reprogramming of WT and *PHF20* KO MEFs transduced with *Ink4a/Arf*- or *p21*-specific or control shRNA. (J) Number of AP-positive colonies counted on day 14 of 4F-mediated reprogramming of WT and *PHF20* knockout MEFs with or without *PHF20* cDNA expression. (K) Western analysis of PHF20 expression in WT and Tet-O-*PHF20* transgenic MEFs expressing *rtTA* in the presence of Dox. AP-positive colonies were counted on day 14 of 4F-mediated reprogramming of *rtTA*-expressing Tet-O-*PHF20* transgenic MEFs. (L) Number of AP-positive colonies counted on day 14 of 4F-mediated reprogramming of WT MEFs transduced with Tet-O-*Jmjd3* or Tet-O-*PHF20* in the presence of Dox until day 10. The data in panels **D**, **F** and **H**-**L** are plotted as means ± SD with indicated significance (*$p < 0.05$, **$p < 0.01$). See also Figure S4.

NIH-PA Author Manuscript

NIH-PA Author Manuscript

NIH-PA Author Manuscript

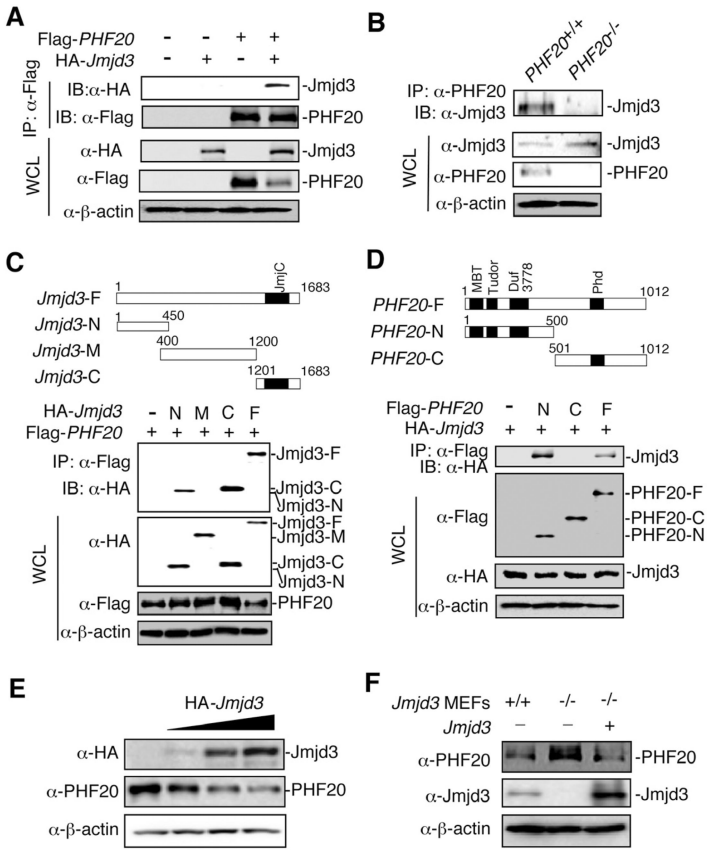


**Figure 5. Jmjd3 Interacts with PHF20 and Causes its Degradation**

(A) 293T cells were transfected with Flag-*PHF20* and HA-*Jmjd3*. Cell extracts were immunoprecipitated with anti-Flag beads, followed by immunoblot (IB) with an anti-HA antibody. (B) Detection of interaction between Jmjd3 and PHF20 in WT and *PHF20* knockout MEFs by immunoprecipitation (IP) with a PHF20 antibody, followed by IB with an anti-Jmjd3 antibody. (C and D) 293T cells were transfected with different HA-*Jmjd3* domain constructs (C) and different Flag-*PHF20* constructs (D). Cell extracts were immunoprecipitated with anti-Flag beads, followed by IB with an anti-HA antibody. (E) 293T cells were transfected with increasing amounts of HA-*Jmjd3* cDNA, followed by IB with anti-PHF20 and anti-HA antibodies. (F) Jmjd3 WT and KO MEF cells were infected with or without Flag-tagged *Jmjd3* retrovirus for24 h, and cell extracts were analyzed by IB with anti-PHF20 and anti-Jmjd3 antibodies. See also Figure S5.

NIH-PA Author Manuscript

NIH-PA Author Manuscript

NIH-PA Author Manuscript

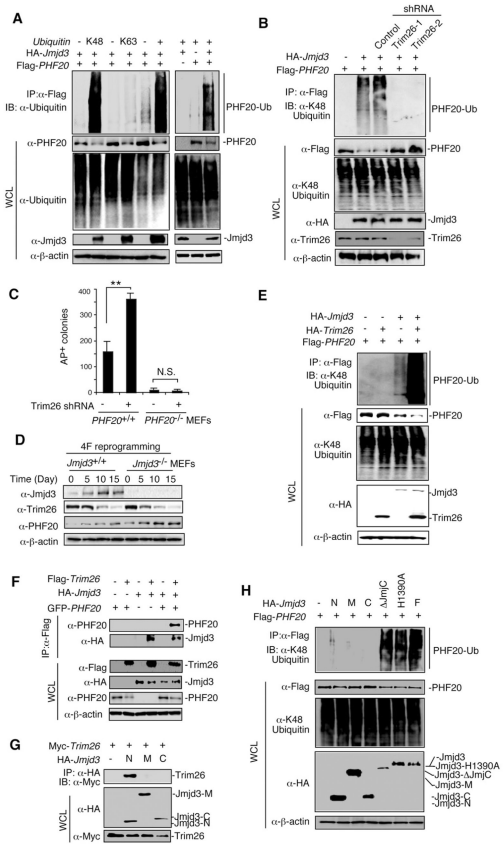


**Figure 6. Jmjd3 Targets PHF20 for Ubiquitination by Recruiting an E3 Ligase Trim26**

(A) 293T cells transfected with HA-tagged *ubiquitin*, Flag-tagged *PHF20* and HA-tagged *Jmjd3*. Cell lysates were immunoprecipitated with anti-Flag beads, followed by IB with an anti-ubiquitin antibody. (B) 293T cells transfected with Flag-tagged *PHF20*, HA-tagged *Jmjd3* and different Trim26 shRNA constructs as indicated. Cell lysates were immunoprecipitated with anti-Flag beads and analyzed with an anti-K48 ubiquitin. (C) Number of AP-positive colonies counted on day 14 of 4F-mediated reprogramming of WT and *PHF20*-deficient MEFs transduced with *Trim26*-specific or control shRNAs. Asterisks indicate significant differences between groups (*$p < 0.05$, **$p < 0.01$, $^{N.S.}$ $p > 0.05$). (D) Western blot analysis of Jmjd3, Trim26 and PHF20 expression in WT and *Jmjd3*-deficient MEFs during cellular reprogramming. (E) 293T cells transfected with HA-*Trim26*, Flag-*PHF20* and HA-*Jmjd3* as indicated. Cell lysates were immunoprecipitated with anti-Flag beads, followed by IB with an anti-K48 ubiquitin antibody. (F) 293T cells transfected with Flag-*Trim26*, *GFP-PHF20* and HA-*Jmjd3* as indicated. Cell lysates were immunoprecipitated with anti-Flag beads, followed by IB with PHF20 and HA antibodies. (G) 293T cells transfected with Myc-*Trim26* and HA-*Jmjd3* constructs. Cell lysates were immunoprecipitated with anti-HA beads, followed by IB with an anti-Myc antibody. (H) 293T cells transfected with Flag-*PHF20* and HA-*Jmjd3* constructs. Cell lysates were immunoprecipitated with anti-Flag beads, followed by IB with an anti-K48 ubiquitin antibody. See also Figure S6.

NIH-PA Author Manuscript
NIH-PA Author Manuscript
NIH-PA Author Manuscript



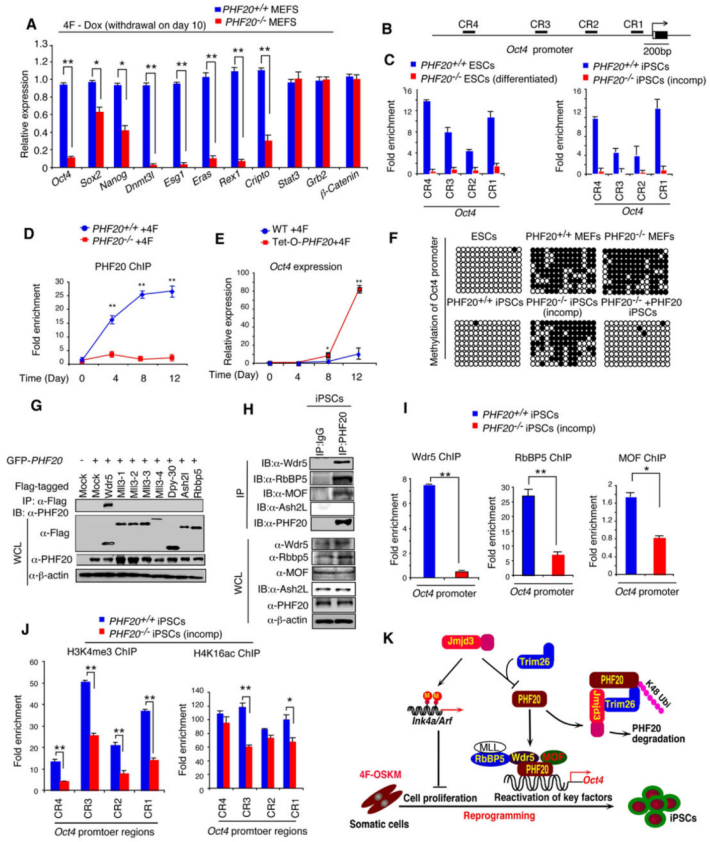


**Figure 7. PHF20 is Required for*Oct4*Expression during Reprogramming by Interacting with Wdr5**

(A) WT and *PHF20* knockout MEFs were reprogrammed by 4F in the presence of Dox for 10 days, followed by Dox withdrawal. Real-time PCR analysis of endogenous *Oct4*, *Sox2*, *Nanog* and other ES genes was performed on day 14. (B) Schematic diagram of *Oct4* promoter regions. (C) Determination of PHF20 binding to the CR regions of *Oct4* promoter in iPSCs and ESCs by ChIP-qPCR analysis with PHF20-specific antibody. Values are reported as fold enrichment relative to input DNA. (D) ChIP-PCR analysis of timing of PHF20 binding to the *Oct4* promoter region during 4F-mediated reprogramming using a PHF20-specific antibody. (E) Real-time PCR analysis of *Oct4* expression in *rtTA*-expressing WT and Tet-O-*PHF20* transgenic MEFs during reprogramming. (F) Bisulfite sequencing of the *Oct4* promoter region in ESCs, PHF20$^{+/+}$ MEFs, PHF20$^{-/-}$ MEFs,iPSCs from PHF20$^{+/+}$ MEFs, iPS-like (incompletely reprogrammed) cells from PHF20$^{-/-}$ MEFs,and iPSCs from PHF20-expressing PHF20$^{-/-}$ MEFs. Open circles (○) stand for unmethylated CpG dinucleotides, while closed circles (•) for methylated CpGs. (G) 293T cells were transfected with *GFP-PHF20*, Flag-tagged *Wdr5*, *MLL3*, *Dpy-30*, *Ash2L* or*Rbbp5*. Cell extracts were immunoprecipiated with anti-Flag beads, followed by IB with an anti-PHF20 antibody. (H) Detection of endogenous interaction between PHF20 and Wdr5 complex in iPSCs by IP with a PHF20 antibody, followed by IB with Wdr5, RbBP5, MOF and Ash2L antibodies. (I) ChIP-qPCR analysis of Wdr5, RbBP5 and MOF binding to *Oct4* promoter region during 4F-mediated reprogramming of WT and *PHF20*-deficient MEFs. (J) ChIP-qPCR analysis of H3K4me3 and H4K16ac mark of the *Oct4* promoter in WT MEF-derived iPSCs and *PHF20*-deficient derived iPSC-like (incompletely reprogrammed) cells. (K) Proposed a working model by which Jmjd3 regulates somatic cell reprogramming. The

data in panels **A**, **C-E**, **I** and **J** are plotted as means ± SD with indicated significance (*p < 0.05, **p < 0.01, by Student's t test). See also Figure S7.

NIH-PA Author Manuscript
NIH-PA Author Manuscript
NIH-PA Author Manuscript